

Original Article

Diagnostic Performance of CT and MRI in Diagnosis of Diseases Involving Pterygopalatine Fossa

Varalee Mingkwansook*, Lalita Chabnak, Thanapat Dechadasawat,
Arvemas Watcharakorn

Abstract

Introduction: To evaluate the diagnostic performance of CT and MRI in diagnosis of pterygopalatine fossa lesions and to describe disease entities involving pterygopalatine fossa (PPF).

Methods: The CT and MRI images of 29 patients who had the PPF lesions were retrospectively reviewed by two neuroradiologists who were blinded to the diagnosis. The radiologist's interpretation was one of four categories; benign soft tissue tumor, malignant soft tissue tumor, primary bone tumor, and inflammatory lesion. The results were compared to final diagnosis and calculated for sensitivity, specificity, accuracy, PPV, NPV, and interobserver agreement.

Results: Of the 29 cases, 18 were malignant soft tissue tumor (62%), 2 were benign soft tissue tumor (7%), 3 were primary bone tumor (10%), and 6 were inflammatory lesion (21%). Benign soft tissue tumor demonstrated highest specificity, accuracy, PPV and NPV (100%). Both benign and malignant soft tissue tumor equaled in highest sensitivity (100%). The interobserver agreement showed substantial agreement (Kappa = 0.744, *P*-value < .001).

Conclusions: CT and MRI have high accuracy in diagnosis of the pterygopalatine fossa lesions with high sensitivity in the detection of benign and malignant soft tissue tumor. However, there was low specificity in diagnosis of the malignant soft tissue tumor because of overlapped findings in malignant tumors and aggressive inflammation.

Keywords: Pterygopalatine fossa, PPF, CT, MRI, Diagnostic performance

Received: 17 September 2021

Revised: 19 October 2021

Accepted: 25 October 2021

Introduction

The pterygopalatine fossa (PPF) is a small space but very important anatomic crossroad at the deep face as it connects between several intra- and extra-cranial compartments including orbit, nasal cavity, nasopharynx, oral cavity, and the middle cranial fossa.¹⁻⁷ Therefore, various etiologies including neoplastic and inflammatory diseases can originate or spread through this area either by direct spread or via neurovascular communications. PPF is bounded by maxillary sinus, palatine bone and pterygoid process of sphenoid bone. Its major contents include pterygopalatine ganglion, maxillary division of trigeminal nerve, vidian nerve, fat, various arteries, and veins.

Computed tomography (CT) and magnetic resonance imaging (MRI) have major role in diagnosis of the diseases involving PPF as this structure is deeply located in the deep face and precise diagnosis would be impossible based-on clinical information alone. CT is known as the best modality to detect bony changes, chondroid and osteoid matrix. MRI is excellent for detection, characterization and determining extension of soft tissue pathologies. Obliteration of fat in the pterygopalatine fossa is the important indicator of pathology.³⁻⁸

Many imaging features aid in distinguishing malignant from benign tumor or inflammatory lesion has been described. Large volume, poorly defined margin and bony invasion may suggestive of malignant soft tissue tumor.⁹ Benign soft tissue masses usually show pressure erosion or scalloping of adjacent bone.¹⁰ Calcified matrix in the lesion should lead to chondroosseous type tumor.⁹ However some findings overlap between benign and malignant conditions. Chronic invasive fungal sinusitis may appear as mass-like lesion with bone destruction and invade adjacent structures which mimic malignant tumor.¹¹

This study expects that this research will reveal the performance of CT and MRI in diagnosis of the various etiologies of the lesions that involve the PPF.

To evaluate the diagnostic performance of CT and MRI in diagnosis of diseases involving PPF and to describe incidence of diseases involving this area.

Methods

Study population

The retrospective study was approved by the ethics committee at the institution. The retrospective chart review by using the keywords: “pterygopalatine fossa” or “PPF” through the radiologic database for CT and MRI examination during the period of January 2017 to December 2019. The inclusion criteria were (a) patient's age over 15-year-old (b) patients with the pterygopalatine fossa lesion who had pretreatment CT or MRI of head and neck (c) patients with pathological or clinical of final diagnosis. Patients who had history of severe traumatic facial injury were excluded from the study. Demographic and clinical data including age, gender, CT or MRI examination parts and date of examination, treatment, operative note and pathological or clinical final diagnosis were collected.

Machines

CT was performed using our institution's routine protocol, acquired with a 256-detector CT scanner (Philips, iCT powered by iPatient), or a 128-detector CT scanner (Siemens, SOMATOM Definition AS). In our study, CT scan was obtained in 25 patients, including both contrast-enhanced CT and non contrast-enhanced CT. There were CT neck, CT orbit, CT paranasal sinuses, CT oral cavity, CT brain and CT facial bone. All CT images covered from skull base to hard palate at least. The images were reconstructed in range of 1 - 5 mm thickness.

The MR examination was performed in 5 patients, using a 1.5 Tesla (Siemens MEGNETOM Aera) or 3 Tesla MRI (Siemens MAGNETOM Skyla). The minimum sequences included T1WI, T2WI, T2-FLAIR, T2*GRE, fat-suppression T1W with gadolinium and diffusion images. The images were displayed by using a PACS workstation.

Imaging interpretation

Each study was retrospectively reviewed by two experienced neuroradiologists independently. Any discrepancies between the two neuroradiologists were resolved by their additional consensus reading. They were blinded to information of individual patient.

The images were diagnosis into one of four categories; benign soft tissue tumor, malignant soft tissue tumor, primary bone tumor, and inflammatory lesion. Results of CT and/or MRI interpretation were compared to the final diagnosis.

Statistical analysis

The sensitivity, specificity, accuracy, positive predictive value (PPV), and negative predictive value (NPV) of CT and MRI for diagnosis of the pterygopalatine fossa lesions were calculated.

The Cohen kappa statistic was used to determine the interobserver agreement.

Results

Demographic data

A total of 29 patients were eligible for this study. Seventeen were males (59%) and twelve were females (41%); range 22 - 86 years, median age was 58 years. There were 24 patients performed CT scan alone and 4 patients had only MRI. Only one patient underwent both CT and MRI. The demographic data was summarized in Table 1.

Table 1 Demographic data

General characteristics		Number	Percentage (%)
Sex			
	Male	17	59
	Female	12	41
Age (years)			
	15 - 30	4	14
	31 - 50	9	31
	More than 50	16	55
Imaging modality			
	CT	24	83
	MRI	4	14
	CT and MRI	1	3

Of the 29 cases, 18 were malignant soft tissue tumors (62%), 2 were benign soft tissue tumors (7%), 3 were primary bone tumors (10%), and 6 were inflammatory lesions (21%). The most

common disease was nasopharyngeal cancer (9 cases, 31%). Details of each disease are showed in Table 2.

Table 2 Final diagnosis

Final diagnosis	Number (total 29)	Percentage (%)
Malignant soft tissue tumor		
Nasopharyngeal cancer	9	31
Lymphoma	3	10
CA maxillary sinus	2	6.9
Malignant round cell tumor	1	3.4
CA hard palate	1	3.4
CA nasal cavity	1	3.4
Metastasis from lung cancer	1	3.4
Benign soft tissue tumor		
Schwannoma	1	3.4
Nasopharyngeal angiofibroma	1	3.4
Primary bone tumor		
Osteosarcoma	1	3.4
Fibrous dysplasia	1	3.4
Ossifying fibroma	1	3.4
Inflammatory lesion		
Fungal sinusitis	4	13.8
Sinusitis, non-specified	1	3.4
Chronic inflammation, non-specified	1	3.4

Interobserver agreement

The overall interobserver agreement showed substantial agreement (Kappa = 0.744, *P*-value < .001).

Diagnosis performance

Calculated sensitivity, specificity, accuracy, precision, and negative predictive value (NPV) for CT and MRI in diagnosis of categories

of pterygopalatine fossa lesions are shown in Table 3. The image diagnosis for benign soft tissue tumor demonstrated the highest specificity and accuracy (100%) and for both benign and malignant soft tissue tumor equaled in the highest sensitivity (100%). The diagnosis for primary bone tumor had the lowest sensitivity (33.3%) and for malignant soft tissue tumor had the lowest specificity (72%).

Table 3 Diagnostic performance of CT and MRI in diagnosis of PPF lesions

Disease categories	Sensitivity	Specificity	Accuracy	Precision	NPV
Benign-soft tissue tumor	100 (2/2)	100 (27/27)	100 (29/29)	100 (2/2)	100 (27/27)
<i>95% CI</i>	15.81 - 100	87.23 - 100	88.06 - 100	-	-
Malignant-soft tissue tumor	100 (18/18)	72 (8/11)	89.7 (26/29)	87.5 (18/21)	100 (8/8)
<i>95% CI</i>	81.47 - 100	39.03 - 93.98	72.65 - 97.81	69.57 - 94.03	-
Primary bone tumor	33.3 (1/3)	96.2 (25/26)	93.1 (27/29)	100 (1/1)	92.9 (26/28)
<i>95% CI</i>	0.84 - 90.57	86.77 - 100	77.23 - 99.15	-	85.38 - 96.66
Inflammatory lesion	66.7 (4/6)	95.7 (22/23)	89.7 (26/29)	80 (4/5)	91.7 (22/24)
<i>95% CI</i>	22.28 - 95.67	78.05 - 99.89	72.65 - 97.81	35.15 - 96.72	72.65 - 97.81

Discussion

In the study, malignant soft tissue tumor was the most common etiology which had highest sensitivity (100%) but lowest specificity (72%) on CT and MRI. In this group, nasopharyngeal carcinoma was the most common disease. They appeared as soft tissue mass arising from nasopharyngeal wall, invading adjacent structures and extending to the pterygopalatine fossa (Figure 1 A, B, and C). Associated bony destruction and pathologic nodes were clues for their malignant behavior. These are similar to previously reported by Ahmed AR et al that imaging suggest malignant soft tissue tumor included large volume, extra-compartmental extension, high T2-weighted MR images, invasion of bone and marked peripheral enhancement.⁹⁻¹⁰

Lymphoma was the second most common disease involving the pterygopalatine fossa in our study (3 from 18 cases of malignant soft tissue tumor). The primary origins were from orbit in two cases and anterior skull base in one case. All

three cases of lymphoma showed isosignal intensity on T1WI, slightly hypersignal intensity on T2WI with restricted diffusion (Figure 1 D, E, and F), corresponding to what was described by Ali RS et al.¹¹

In our study, there was no false negative for malignant soft tissue tumor but there were three cases with false positive which were primary bone tumor (chondroblastic osteosarcoma) and inflammatory lesion (invasive aspergillosis rhinosinusitis and chronic inflammation; non-specified).

In case of chondroblastic osteosarcoma (Figure 1 G, H, and I), lesion appeared as a soft tissue mass epicenter at right maxilla with invasion to adjacent structures and bony destruction. There was no internal chondroid or osteoid matrix in this case. Osteosarcoma has been reported of presence of osteoid matrix in 90% of cases by Pablo NB et al.¹² So, in minority cases, osteoid matrix may not be found and might be difficult to diagnosis from other malignant tumor.

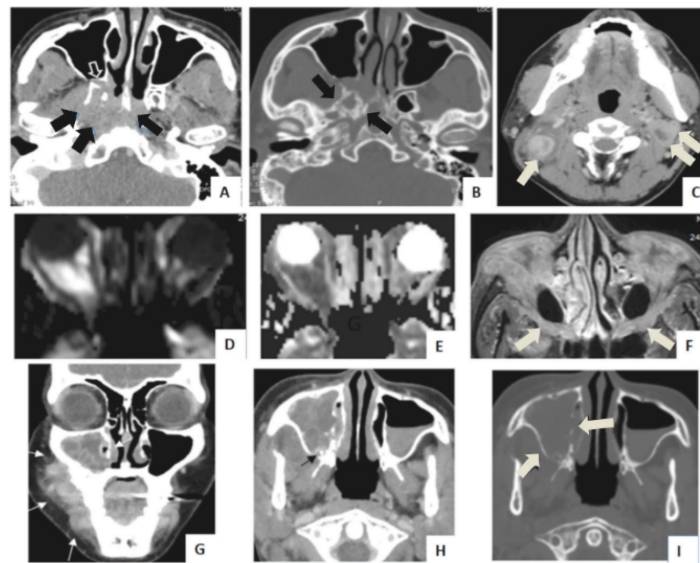


Figure 1 A, B and C: A 40-year-old man with nasopharyngeal squamous cell carcinoma. This was correctly categorized as malignant soft tissue tumor. There is an ill-defined soft tissue tumor epicenter at right-sided nasopharynx (arrow in A) and right PPF (open arrow in A) with bone destruction at right pterygoid bone (arrow in B). Several metastatic nodes at bilateral upper neck (arrow in C) confirm its malignant nature.

D, E and F: A 64-year-old man with extranodal marginal zone B cell lymphoma which was correctly diagnosed as malignant soft tissue tumor. The mass involves both orbits and PPF which show typical restricted diffusion (high signal in D and low signal in E) and rather homogeneous enhancement (F). Rather enlarged bilateral PPFs is also noted (arrow in F).

G, H and I: A 25-year-old woman with chondroblastic osteosarcoma at right-sided maxilla which was interpreted as malignant soft tissue tumor. The mass appears as an enhancing soft tissue mass at right maxillary sinus (arrow in G, H) and causes bony destruction (open arrow in I). No chondroid or osteoid matrix was presented.

A case of invasive aspergillosis rhinosinusitis (Figure 2 A, B, and C), which interpreted as malignant soft tissue tumor, appeared as a soft tissue mass with central enhancement and the epicenter at right orbital apex involving right pterygopalatine fossa. Adjacent bony destruction was presented. These would be unable to differentiate from malignant soft tissue tumor, similar to that described by Manohar A et al.¹³

The third case of false positive for malignant soft tissue tumor was chronic inflammation of right orbital apex (unidentified pathogen) (Figure 2 D, E, and F). The imaging showed a small infiltrative lesion involving left orbital apex, left pterygopalatine fossa and left pterygomaxillary fissure with equivocal enhancement and adjacent

bony destruction. As its aggressive behavior and limited measurement of contrast enhancement due to its small size, this is hard to distinguish between tumor and aggressive inflammation.

There were two benign primary soft tissue tumors in this study, schwannoma and nasopharyngeal angiofibroma. The benign soft tissue tumor exhibited 100% sensitivity, specificity, accuracy, PPV, and NPV.

In case of schwannoma, the mass epicenter at right masticator space, extending to pterygopalatine fossa (Figure 2 G and H). It showed heterogeneous enhancement with bone remodeling and widening of skull base foramina which are typical hallmarks for benign slow growing tumor, similar to previous described by Ty KS et al.¹⁴

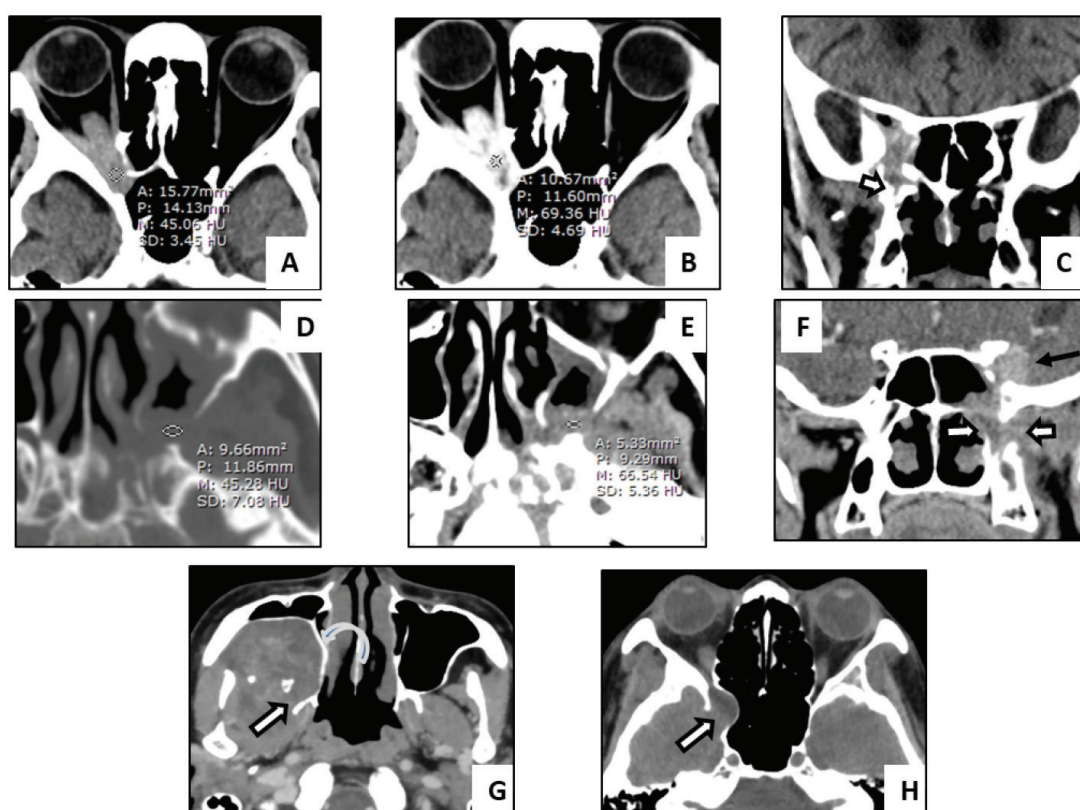


Figure 2 A, B and C: A 80-year-old man with invasive aspergillosis rhinosinusitis was interpreted as malignant soft tissue tumor. The lesion shows isodense on non-contrast CT (A) with solid contrast enhancement (B and C) at right orbital apex and PPF with adjacent bony destruction (arrow in C). D, E and F: A 50-year-old woman with chronic inflammation (unidentified pathogen) was interpreted as malignant soft tissue tumor. The lesion appears as an ill-defined enhancing mass (D and E) at left PPF (open arrow in F) and left cavernous sinus (arrow in F) with bony destruction. G and H: A 47-year-old woman with schwannoma was interpreted as benign soft tissue tumor. There is a heterogeneous enhancing mass at right masticator space with bone remodeling of right maxillary sinus (curve arrow in G) with widening of right PPF (open arrow in G) and inferior orbital fissure (open arrow in H)

Another benign primary soft tissue tumor was nasopharyngeal angiofibroma, epicenter at left posterior nasal cavity with small tumor extension to left sphenopalatine foramen and left pterygopalatine fossa (Figure 3 A, B, and C). It showed typical avid enhancement and foraminal extension. Bony remodeling was not presented in this case due to its small size.

There was high specificity (92.9%) but has low sensitivity (33.3%) for primary bone tumor. Fibrous dysplasia at pterygomaxillary bones was correctly diagnosed which showing typical expansile lesion, ground glass attenuation and intact bony cortex (Figure 3 D). These findings were identical to described by Peterson RB et al.²

The two cases of primary bone lesion that were diagnosed as inflammatory lesion and primary malignant soft tissue tumor, respectively. A case of ossifying fibroma (Figure 3 E and F), there was a mixed soft tissue-calcific content lesion and the epicenter at right ethmoid sinus and right nasal cavity involving right pterygopalatine fossa. It showed no definite solid enhancing portion. The calcification in this case did not show characteristic of osteoid or chondroid matrix. These findings could mimic fungal infection. Another case of primary malignant bone lesion was osteosarcoma which interpreted as primary malignant soft tissue tumor due to absence of osteoid matrix as stated above (Figure 1 G, H, and I).

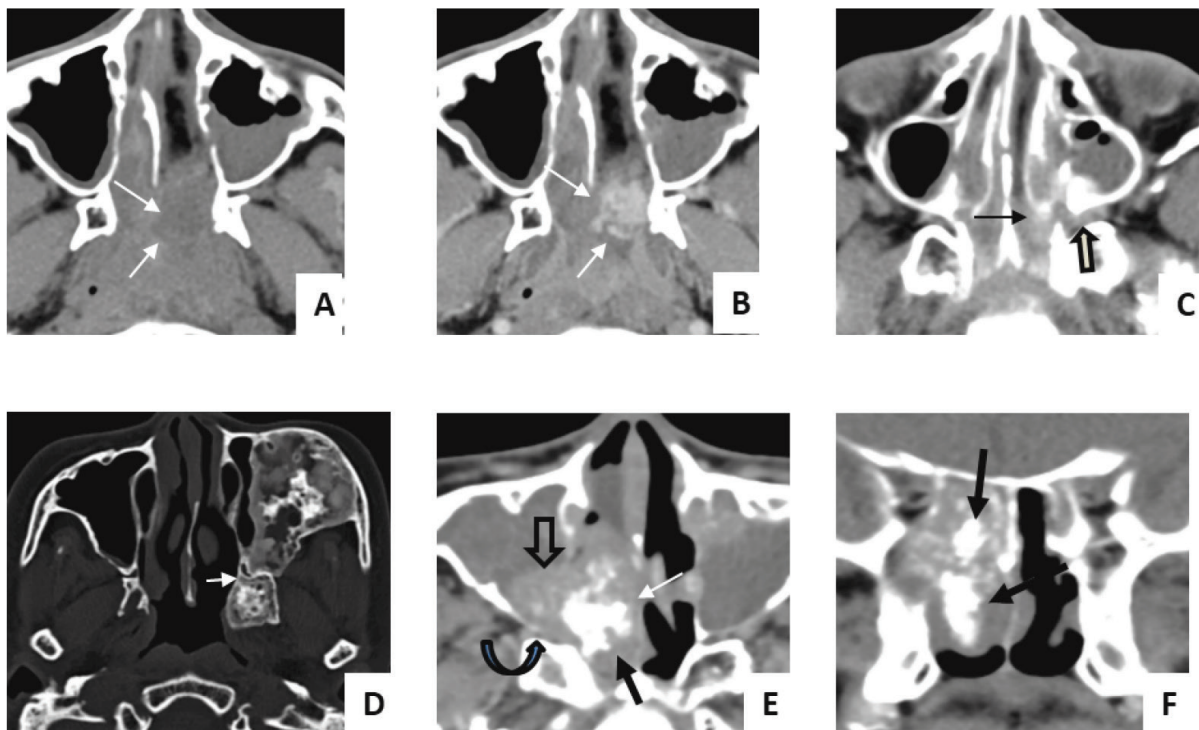


Figure 3 A, B and C: A 22-year-old man with nasopharyngeal angiofibroma was interpreted as benign soft tissue tumor. There is a marked enhancing mass at left posterior nasal cavity (arrow in A and B). It involves left sphenopalatine foramen (arrow in C) and left PPF (open arrow in C). D: A 67-year-old woman with fibrous dysplasia at pterygomaxillary bone involving left PPF (arrow in D) was interpreted as primary bone tumor. E and F: A 74-year-old woman with ossifying fibroma was interpreted as inflammatory lesion. There is an enhancing lesion (open arrow in E) at right nasal cavity involving PPF with adjacent bony destruction (curve arrow in E). Its internal hyperdense content (arrow in E and F) mimic fungal infection.

The group of inflammatory lesion revealed high specificity (95.7%) but low sensitivity (66%). There were four cases of true diagnosis, two were fungal ball, one was invasive fungal sinusitis and the other was sinusitis with unidentified pathogen. Two cases of fungal ball showed high attenuating soft

tissue lesion in non-contrast CT which located at paranasal sinus with fat haziness at pterygopalatine fossa and exhibited sclerotic wall of sinus (Figure 4 A and B), similar to that described by Manohar A et al.¹²

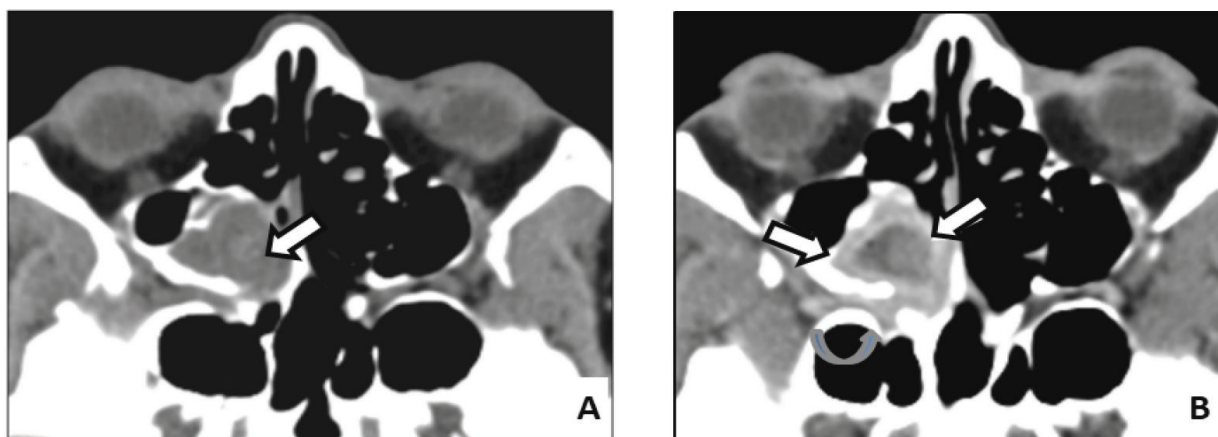


Figure 4 A and B: 58-year-old man with fungal ball at right ethmoid sinus was interpreted as inflammatory lesion. There is a hyperattenuating content (open arrow in A) with mucosal thickening at right posterior ethmoid sinus (open arrow in B) with fat haziness and increased enhancement at right PPF (curve arrow in B).

There were two cases of inflammatory lesion (invasive fungal rhinosinusitis (Figure 2 A, B, and C) and chronic inflammation of orbital apex, unidentified pathogen, (Figure 2 D, E, and F) that diagnosed as malignant soft tissue tumor. Both cases appeared as a soft tissue mass involving pterygopalatine fossa with adjacent bony destruction which difficult to distinguish between malignant soft tissue tumor and inflammatory condition, as discussed earlier.

The limitation in our study is due to small population size as all of the lesions involving pterygopalatine fossa in our study arise from neighbouring spaces. Thus, the lesion must be sufficient extensive to be included in this study. There is also scarcity of MRI in this study, so the further study with larger population of MRI in disease involving pterygopalatine fossa might have more information to better evaluate the diagnostic performance.

In conclusion, CT and MRI have high accuracy in diagnosis of the disease involving pterygopalatine fossa in all disease categories with high sensitivity in detection of benign and malignant soft tissue tumor. However, CT and MRI

might show limited diagnosis (72% specificity) in malignant soft tissue tumor, particular for the early cancer as this disease category might have some overlap findings with aggressive inflammatory condition. Fungal infection is also a great mimicker of both malignant soft tissue mass or primary bone tumor due to their various calcified pattern and invasiveness. Thus, radiologists should be aware of interpreting CT and MRI of disease involving pterygopalatine fossa.

Acknowledgments

Financial support. None reported.

Potential conflicts of interest. All authors report no conflicts of interest relevant to this article.

References

1. Yu Q, Wang P, Shi H, Luo J, Sun D. The lesions of the pterygopalatine and infratemporal spaces: Computed tomography evaluation. *Oral Surg Oral Med Oral Pathol Oral Radiol Endod.* 1998;85(6):742-751. doi: 10.1016/s1079-2104(98)90045-2.

2. Peterson RB, Lorenzo G, Desai NK. Pterygopalatine fossa masses in children: oh, the places they'll go. *Neurographics*. 2016; 6:1-15. doi: 10.3174/ng.1160137.
3. Tomura N, Hirano H, Kato K, et al. Comparison of MR imaging with CT in depiction of tumour extension into the pterygopalatine fossa. *Clin Radiol*. 1999;54(6):361-366. doi: 10.1053/crad.1999.0179.
4. Tashi S, Purohit BS, Becker M, Mundada P. The pterygopalatine fossa: imaging anatomy, communications, and pathology revisited. *Insights Imaging*. 2016;7(4):589-599. doi: 10.1007/s13244-016-0498-1.
5. Derinkuyu BE, Boyunaga O, Oztunali C, Alimli AG, Ucar M. Pterygopalatine Fossa: Not a Mystery! *Can Assoc Radiol J*. 2017;68(2):122-130. doi: 10.1016/j.carj.2016.08.001.
6. Tashi S, Purohit BS, Becker M, Mundada P. The pterygopalatine fossa: imaging anatomy, communications, and pathology revisited. *Insights Imaging*. 2016;7(4):589-599. doi: 10.1007/s13244-016-0498-1.
7. Erdogan N, Unur E, Baykara M. CT anatomy of pterygopalatine fossa and its communications: a pictorial review. *Comput Med Imaging Graph*. 2003;27(6):481-487. doi: 10.1016/s0895-6111(03)00038-7.
8. Al Shehri F. M.R.I diagnosis of tumours and tumour-like conditions affecting the pterygopalatine fossa. *Int J Health Sci (Qassim)*. 2013;7(2):124-128. doi: 10.12816/0006035.
9. Razek AA, Huang BY. Soft tissue tumors of the head and neck: imaging-based review of the WHO classification. *Radiographics*. 2011;31(7):1923-1954. doi: 10.1148/rg.317115095.
10. Abdel Khalek Abdel Razek A, King A. MRI and CT of nasopharyngeal carcinoma. *AJR Am J Roentgenol*. 2012;198(1):11-18. doi: 10.2214/AJR.11.6954.
11. Sepahdari AR, Aakalu VK, Setabutr P, Shiehorteza M, Naheedy JH, Mafee MF. Indeterminate orbital masses: restricted diffusion at MR imaging with echo-planar diffusion-weighted imaging predicts malignancy. *Radiology*. 2010;256(2):554-564. doi: 10.1148/radiol.10091956.
12. Pablo NB, Paloma MM, Jaid FL. ASNR. Osteosarcoma of the maxillary sinus. <http://www.Ajnr.org/ajnr-case-collections-diagnosis/osteosarcoma-maxillary-sinus>. published 2018. Accessed 2021.
13. Aribandi M, McCoy VA, Bazan C. Imaging features of invasive and noninvasive fungal sinusitis: a review. *Radiographics*. 2007; 27(5):1283-1296. doi: 10.1148/rg.275065189.
14. Subhawong TK, Fishman EK, Swart JE, Carrino JA, Attar S, Fayad LM. Soft-tissue masses and masslike conditions: what does CT add to diagnosis and management? *AJR Am J Roentgenol*. 2010;194(6):1559-1567. doi: 10.2214/AJR.09.3736.